Cation–Cation Interactions in Neptunium(V,VI)-diglycolamide System

Christelle Tamain, Matthieu Autillo, Dominique Guillaumont, Luca Briscese, Claude Berthon

Cation-cation interactions in Neptunium(V,VI)-diglycolamide system

Christelle TAMAIN*, Matthieu AUTILLO, Dominique GUILLAUMONT, Luca BRISCESE, Claude BERTHON

CEA, DES, ISEC, DMRC, Univ Montpellier, Marcoule, France

Corresponding author: christelle.tamain@cea.fr

Abstract

SC-XRD structure and Raman spectra of two new mixed-valence Np(V)-Np(VI) compounds with cation – cation interactions (CCIs) using TEDGA (TetraEethylDiGlycolAmide, belonging to the diglycolamide family), as a ligand are reported: a trimeric species, $[Np^{V}O_2(TEDGA)_2]_2[Np^{VI}O_2(NO_3)_2](NO_3)_2$ (**1**), which is the first neptunium representative of a linear actinide trimer with CCIs, and a dimeric species, $[Np^{V}O_2(TEDGA)_2][Np^{VI}O_2(NO_3)_3].CH_3CN$ (**2**). These two structures were prepared thanks to controlled and reproducible syntheses, based on the mixing of the two monomers solutions in an inert solvent: a Np(V)-TEDGA monomer solution mixed with a dinitrate or trinitrate Np(VI) solution. To better understand the impact of the CCIs on the actinyl cations electronic properties, these structures were compared to the constituent monomers, $[Np^{V}O_2(TEDGA)_2]^{+}$ (**3**) that was also synthesized and $Np^{VI}O_2(NO_3)_2(H_2O)_2$. To complete the series, the $[Np^{VI}O_2(TEDGA)_2]^{2+}$ (**4**) monomer is also reported. In addition, DFT calculations were performed to aid in interpreting the Raman experimental data, to characterize the bonding in such polynuclear species and to identify the main parameters influencing the stability of cation-cation structures, such as the nature of counter ions, the influence of alkyl chains and the presence of weak intra- or intermolecular interactions.

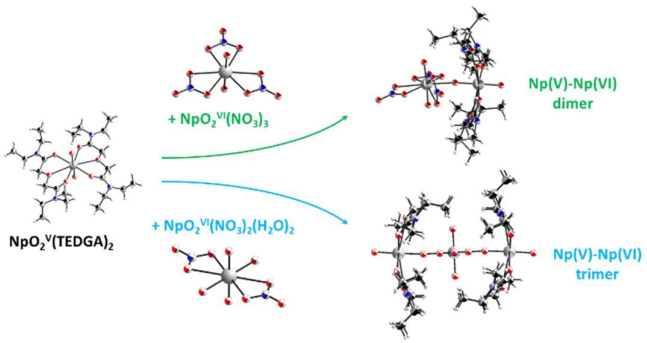

Introduction

The actinide (An) chemistry is mostly influenced by the formation of polynuclear species that have attracted valuable interest over the last decades. These species have been proven to play an important role in the waste management, fuel reprocessing and even in biological media.[1,2,3,4] There are several ways to connect actinides: the complexation through polydentate bridging ligands, named coordination polymer, the hydrolysis/condensation of actinide leading to the formation of variable oxo-hydroxo

bridged complexes, named clusters,[2] and compounds with cation–cation interactions (CCIs). All these species, underestimated in actinide speciation, can have a major influence on actinide speciation, chemistry and reactivity. For example, we recently redefined the speciation diagram of the Pu-acetate system with the dominated presence of a hexameric complex formed in a wide range of chemical conditions, whereas none of the previous studies mentioned this polynuclear species.[5] In liquid-liquid extraction, it is also known that CCI compounds also drastically modify the actinide separation behavior and performances. For instance, the formation of Np(VI)-Np(V), U(VI)-Np(V), Pu(IV)-Np(V) or U(VI)-Tc(VII) CCIs complexes is known to increase the unwanted extraction of neptunium or technetium during liquid-liquid extraction by TriButylPhosphate (TBP) or monoamide (DEHiBA).[6,7]

The CCI in actinide science is defined as the interaction between the axial oxygen of an actinyl (trans-dioxo AnO_2^{n+} cation) and another cationic center. The yl bond is particularly strong due to the presence of both σ and π interactions between 5f and 6d orbitals of the metal center and the O 2p orbitals.[8,9] The coordination in the equatorial plane of the actinyl ion by one or several ligands weaken the yl bond increasing the Lewis base character of the oxo group.[7,10,11] This property is exacerbated for +V oxidation state explaining why they are most involved in CCI compounds. Beyond its nuclear industrial interest, CCIs have also a critical role in material science with the enhancement of magnetic interactions giving rise to the formation of magnets.[12,13] Furthermore, in more fundamental researches, CCIs are also involved in mechanism as intermediate steps in actinide redox chemistry and disproportionation reactions.[14,15,16,17]

The coordination modes versatility differing in the number of cations involved, the shape of the molecular structure (linear or not) and the oxidation state of the doner or acceptor actinides,[18] are responsible for the multiplicity of the solid structure arrangements.[19] CCI compounds exhibit diverse metal-ion lattice connectivities ranging from discrete molecules to coordination polymers with various dimensions: chains or ribbons (1D), layers (2D) or 3D-networks. Numerous extended structures containing CCIs with association of one or several An oxidation states were described in the literature. In this paper, we are interested only in discrete compounds with finite and small nuclearities (number of actinide atoms involved in the structure, N). Structures with N from 2 to 5 were reported in the literature. Single-valence dimers were described for An(V) (with An = Np[20, 21, 22, 23, 24] or U[25,17]) and U(VI)[26,27]. The U(V)-U(VI)[28] and Np(V)-Np(VI)[9] dimers are the only representatives of mixed-valence complexes containing only two actinides. All these dimers made only of actinyls can be further grouped into two distinct categories according to the geometry in diamond- or T-shape. For N=3, single-valence trimers were synthesized and characterized for U(VI)[16,29,30,31] and An(V) (with An = U[32], Np[33] or Pu[34]). Trimers presenting several oxidation states were described for An(IV)-An(V) (with An = Np[35] or U[36]), An(V)-An(VI) (with An = Np[37] or U [28]) systems. The predominant shape of these trimers is a triangle with an actinide located at every vertex and connected to the two others.[28,29,33,34] Two other geometries can be observed: the first one seems like an opened triangle with one side missing (i.e. a bent line)[35,37]

and a linear arrangement with three aligned actinide cations[36]. Tetramer units were largely described as a more or less distorted square for An(IV)-An(V) (with An=Np[35,38] or U[39]), An(V) (with An=U[17,13,40,41] or Np[42,43]), U(VI)[16,44] and U(V)-U(VI).[40] A few of them were reported with particular symmetries.[35,38,39] Finally, above the nuclearity of 4, only one study reports the formation of a pentamer for the U(IV)-U(V)[39] system.

With its versatile chemistry and the possibility to stabilize three different oxidation states (+IV, +V and +VI) in nitric acid solutions, the neptunium cation is particularly affected by these cation-cation interactions.[45] We report here the second mixed-valence neptunium Np(V)-Np(VI) trimer, $[Np^{V}O_2(TEDGA)_2]_2[Np^{VI}O_2(NO_3)_2](NO_3)_2$ (**1**), which is the first neptunium representative of a linear actinide arrangement, and a Np(V)-Np(VI) dimer, $[Np^{V}O_2(TEDGA)_2][Np^{VI}O_2(NO_3)_3].CH_3CN$ (**2**), both stabilized by TEDGA (TetraEthylDiglycolAmide) ligand. The linear geometry of the trimer (**1**) was described only for two oligomers: one U(VI)[29] and one U(VI)-U(V)[36] compounds. TEDGA belongs to the family of diglycolamides, which are molecules of interest in actinide separation, since their long-chain alkyl representatives are potential extractants for advanced separation,[46, 47, 48, 49,50, 51] and their short-chain representatives are being studied as complexing agents in the aqueous phase for the separation of minor actinides.[52, 53, 54, 55] These two structures were prepared thanks to controlled and reproducible syntheses based on the mixing of the two monomers solutions in an inert solvent: Np(V)-TEDGA monomer solution mixed with a dinitrate or trinitrate Np(VI) solution. The solid compounds were characterized by SC-XRD and Raman spectroscopy. To better understand the impact of cation-cation interactions on the actinide electronic structure, trimer **1** and dimer **2** compounds were compared to the monomers constituting their structures, $[Np^{V}O_2(TEDGA)_2]^{+}$ (**3**) and $[Np^{VI}O_2(NO_3)_2(H_2O)_2]$.[56] The $[Np^{VI}O_2(TEDGA)_2]^{2+}$ (**4**) monomer is also reported and described. For this last compound, it was synthesized from a perchlorate media instead of a nitrate media (media used for structures **1**, **2** and **3**) for stability reasons: the synthesis in nitrate media led to a partial reduction of the neptunium(VI). In addition to describing new structures and contributing to the development of fundamental research, this study also allows acquiring reference spectra (Raman and Vis-nIR spectra) that will enable these compounds to be easily identified in forthcoming liquid-liquid extraction experiments. To support the experiments, DFT calculations were performed to aid in interpreting the experimental data (particularly the Raman spectra), to characterize the bonding in such polynuclear species and to identify the main parameters influencing the stability of these cation-cation structures, such as the nature of counter ions, the influence of alkyl chains and the presence of weak intra- or intermolecular interactions.

Experimental part

^{237}Neptunium precursors are radioactive and chemically toxic reactants, so precautions with suitable care and protection for handling such substances have been followed. The manipulation of these

elements has been carried out at the ATALANTE facility (CEA-ISEC, France). Because of their highly radioactive nature, the experiments were carried out in a regular air atmosphere negative pressure glove box with restrictive protocols.

Chemicals – The neptunium starting material is solid $Np^{V}O_2OH$. Silver (+II) oxide ($Ag^{II}O$), silver trifluoromethanesulfonate, ($AgCF_3SO_3$), nitric acid (HNO_3) 65%, hydrochloric acid (HCl) 37%, perchloric acid ($HClO_4$) 70%, tetrahydrofuran (THF), diisopropyl ether ($(CH_3)_2CH_2O$), acetonitrile (CH_3CN), tetraethymammonium chloride (TEACl) and sodium nitrite ($NaNO_2$) were purchased from Sigma-Aldrich. TEDGA was provided by Pharmasynthese (Lisses, France).

Oxidation of Np(V) to Np(VI) – Solutions of Np(V) in HNO_3, formed by dissolution of $Np^{V}O_2OH$ in 3 $mol.L^{-1}$ HNO_3, were oxidized by addition of $Ag^{II}O$ (10 eq). The Np(VI) oxidation state was checked by Visible-nIR spectrophotometry. The Ag^{+} ion were then precipitated by addition of a stoichiometric amount of HCl (Ag:Cl 1:1) and the solution was separated from the AgCl precipitate by centrifugation.

Neptunium(VI) precursor synthesis – $[(C_2H_5)_4N]_2[Np^{VI}O_2(Cl)_4]$ – A Np(VI) nitric acid solution (prepared as presented above) was successively evaporated under N_2 (×3) with addition of HCl 37% to remove residual nitric acid. The resulting solid of the last evaporation was dissolved in HCl 37% and 2 equivalents of tetraethylammonium chloride (TEACl) was added. The evaporation of the solution induces the precipitation of $[(C_2H_5)_4N]_2[Np^{VI}O_2(Cl)_4]$. The solid was washed with tetrahydrofuran several times and dried at room temperature under N_2.

Np(V)–TEDGA monomer (**3**) *synthesis* – $[(C_2H_5)_4N]_2[Np^{VI}O_2Cl_4]$ was dissolved in CH_3CN (m_{Np}= 10 mg, V = 1 mL). To remove the chloride anions, solid $AgCF_3SO_3$ was added with a molar ratio $[(C_2H_5)_4N]_2[Np^{VI}O_2Cl_4]$:$AgCF_3SO_3$ of 1:4 and the resulting AgCl precipitate was removed by centrifugation. The reduction of the Np(VI) to Np(V) was achieved by addition of $NaNO_2$ (4 eq, m_{NaNO2}= 11.6 mg). The reduction induces the precipitation of a pale green solid, which was isolated from the solution by centrifugation. A slight excess of TEDGA (molar ratio Np:TEDGA of 1:2.2) diluted in CH_3CN was added directly on the solid. After several hours, the solid got dissolved and the Visible-nIR absorption spectrum confirmed the complexation of Np(V) by the TEDGA ligands. Diisopropyl ether diffusion led to the formation of $[Np^{V}O_2(TEDGA)_2].NO_3.2H_2O$ (**3**).

Np(VI) –TEDGA monomers (4) synthesis – The Np(VI) precursor, $[(C_2H_5)_4N]_2[Np^{VI}O_2Cl_4]$, was dissolved in CH_3CN (mNp= 10 mg, V= 500 µL) containing four equivalents of silver triflate inducing the precipitation of AgCl. After removing of AgCl by centrifugation, the addition of two equivalents of TEDGA and two equivalents of $NaClO_4$ to the solution followed by a slow evaporation allowed the formation of crystals of $[Np^{VI}O_2(TEDGA)_2].2ClO_4$ (**4**).

Trimer (1) synthesis – A solution of Np(V)-TEDGA complex was prepared according to the protocol described for the Np(V)–TEDGA monomer (**3**) synthesis (m_{Np}= 10 mg). Aside, a solution of Np(VI)

dinitrate complex (mNp= 5 mg, V= 500 µL) was prepared after dissolution in CH_3CN of the $NpO_2(NO_3)_2(H_2O)_2.H_2O$ solid prepared following existing procedure.[56] The two solutions were mixed together. The resulting solution was concentrated and crystals slowly crystallized using diisopropyl ether liquid-gas diffusion. Crystals, green needles, suitable for SC-XRD were isolated and identified as the $[Np^{V}O_2(TEDGA)_2]_2.[Np^{VI}O_2(NO_3)_2].(NO_3)_2$ (**1**) trimer.

Dimer (2) synthesis – A solution of Np(V) with a slight excess of TEDGA was prepared according to the protocol described for the Np(V)–TEDGA monomer (**3**) synthesis (m_{Np}= 5 mg). Aside, a solution of Np(VI) trinitrate complex (mNp= 5 mg, V= 500 µL) was prepared after dissolution in CH_3CN of the $(TEA)NpO_2(NO_3)_3$ solid prepared following existing procedure.[56] The two solutions were mixed together with a one to one ratio between Np(V) and Np(VI) and the resulting solution was slowly evaporated. Crystals, green prisms, suitable for SC-XRD were isolated and identified as corresponding to the $[Np^{V}O_2(TEDGA)_2].[Np^{VI}O_2(NO_3)_3].CH_3CN$ (**2**) dimer.

SC-XRD – Crystals were mounted on Micro-Mount patented by MiTeGen, inserted into a goniometer base. To prevent actinide health hazards, a MicroRT capillary was then drawn over the sample and onto the base, where it was sealed by adhesive. For crystals **1**, **2,** and **3,** the single crystal XRD intensities were measured on a Bruker D8 Quest diffractometer equipped with a Photon II detector coupled device at 100 K, using a 800 series cryostreamcooler (Oxford Cryosystem). The instrument was equipped with a Mo-target IµS Microfocus source (lambda = 0.71073 Å). The single crystal XRD intensities of crystal **4** were measured on Mo-K_α radiation on a Nonius four circle diffractometer equipped with a Bruker Apex2 detector coupled device at 150 K, using a 600 series cryostreamcooler (Oxford Cryosystem). For all the structures, data were collected using phi and omega scans. Intensities were extracted from the collected frames using the program SAINTPlus.[57] The unit cell parameters were refined from the complete data set, and a multi-scan absorption correction was performed.[58] The structure determination and refinement were realized with Shelx-2017 software.[59] The heavy atoms were located by direct methods while the remaining atoms were found from successive Fourier map analyses. All of the non-hydrogen atoms were located and their positions were refined anisotropically. Hydrogen atoms of the TEDGA molecules were placed in calculated positions refined using idealized geometries (riding model) and assigned fixed isotropic displacement parameters. The hydrogen atoms of the water molecules were placed from Fourier map analyses with O-H distances restrained to 0.8 Å and refined with isotropic displacement parameters. The main crystal data and details of the final refinement are reported in Table 1. Structures were deposited on CCDC structural database with numbers from 2412071 to 2412074.

Table 1: Summary of Crystallographic Data Collection and Structure Refinement for the different structures **1**, **2**, **3** and **4**.

	1	**2**	**3**	**4**
CCDC	2412071	2412072	2412073	2412074
	$[Np^{V}O_2(TEDGA)_2]_2\,[Np^{VI}O_2(NO_3)_2].2NO_3$	**$[Np^{V}O_2(TEDGA)_2]\,[Np^{VI}O_2(NO_3)_3].CH_3CN$**	**$[Np^{V}O_2(TEDGA)_2].NO_3.2H_2O$**	**$[Np^{VI}O_2(TEDGA)_2].2ClO_4$**
Formula	$C_{48}\,H_{96}\,N_{12}\,Np_3\,O_{32}$	$C_{26}\,H_{51}\,N_8\,Np_2\,O_{19}$	$C_{24}\,H_{43}\,N_5\,Np\,O_{13}$	$C_{24}\,C_{l2}\,N_4\,Np\,O_{16}$
Crystal size	80 x 20 x 30 µm	120 x 100 x 80 µm	240 x500 x120 µm	100x30x20 µm
Shape and color	Green needle	Green prism	Light-green prismatic plate	Dark-red rods
Crystal system	Triclinic	Triclinic	Monoclinic	Monoclinic
Space group	P-1	P-1	$P2_1/n$	C2
FW ($g.mol^{-1}$)	2064.36	1253.74	846.63	908.18
Density ($Mg.m^{-3}$)	1.920	2.059	1.686	1.668
µ (mm^{-1})	4.423	5.194	3.161	3.090
Temperature	100K	100K	100K	150K
a, Å	12.0471(5)	12.8810(6)	13.8913(5)	16.7734(9)
b, Å	12.5036(6)	13.9484(6)	15.4272(6)	12.7190(6)
c, Å	13.7833(6)	14.7163(6)	16.7452(7)	8.6725(4)
alpha,°	77.825(1)	95.171(1)	-	-
beta, °	84.816(2)	114.486(1)	110.732(1)	102.275(2)
gamma,°	61.6290(1)	116.695(1)	-	-
V, $Å^3$	1786.6(1)	2021.8(1)	3356.2(2)	1807.9(2)
Z	1	2	4	2
final R indices [I > 2σ(I)]	0.0338/0.0410	0.0225/0.0242	0.0248/0.0284	0.0328/0.0355
R indices (all data)	0.0802/0.0841	0.0640/0.0670	0.0726/0.0798	0.0737/0.0765
goof	1.059	1.035	0.969	1.040
2Θ range (°)	3.02-30.52	2.90-30.53	3.11-27.53	2.41-32.15
L.S. parameters, *p*	438	505	415	215
No. of restraints, *r*	6	0	0	3

Raman spectroscopy - A Jobin−Yvon LabRam Raman 242 spectrometer was used in conjunction with a nuclearized superhead (Optique Peter, Lyon, France) mounted on a support with an objective turret (10x, 20x and 50x). The spectrometer was equipped with a YAG laser (100 mW, 532 nm) with a variable filter to provide low-excitation-beam power levels. The superhead was mounted in a glove box, while the Raman spectrometer and laser were installed outside with a fiber-optic signal transmission line. The microscope objective used for single crystal analyses was 20x. Spectra were registered with several laser powers to ensure the compound did not degrade during analysis.

Computational details - DFT calculations were performed using Gaussian 16 package[60] using B3LYP and a dispersion-corrected form B3LYP-D3.[61,62] For neptunium, core electrons were represented by a small core Stuttgart-Cologne Relativistic Effective Core Potentials (RECPs) along with the associated TZ-valence basis set.[63,64] For other atoms, the 6-31G+(d,p) basis-set was used. Unless stated otherwise, calculations were performed in the gas phase. If present, solvation effects were accounted for through an IEF-PCM continuum model for water as implemented in Gaussian 16. The ground state character of the wavefunction was checked using the stable keyword in Gaussian. Optimized geometries were confirmed to be true minima by frequency calculations (no imaginary values were found). Atomic coordinates are given in SI (SI-xyz file).

Visible spectroscopy - The actinide solutions were analyzed by Vis-nIR absorption spectroscopy between 400 and 1300 nm using a Cary 5000 UV spectrophotometer (Agilent) equipped with glass fibers to allow analyses in gloves box. Solid spectra were collected using a Shimadzu UV2600 spectrophotometer equipped with an integration sphere. The data were registered in reflectance mode with powder stuck between two crystal tapes. The spectra of the compounds **1**, **2**, **4** and of solution prior to crystallization of **3** are given figures S2, S3 and S4 in SI (SI-XRD-UV-DFT file).

Results and discussion

Structure description

Monomers structural description - The Np(V) monomer (**3**), $[Np^{V}O_2(TEDGA)_2].NO_3.2H_2O$, was described in the monoclinic system with $P2_1/n$ space group. The oxidation state of the neptunium was checked with BVS (bond valence sum[65,66,67]) values of 5.02 or 5.03 depending on parameters used for Np–O bonds[68,69,15] (see table S1 in SI for more details - SI-XRD-UV-DFT file). The coordination sphere of the neptunyl unit is composed by two tridentate TEDGA ligands coordinated in the equatorial plane through the two carbonyl functions and the central ether group (see figure 1). With an angle of 178.6(1)° and distances of 1.838(2) and 1.804(2) Å, the yl linear moiety is in agreement with the literature regarding Np(V) structures, i.e. a Np=O bond in the 1.795-1.864 Å range ($<Np=O>_{average}$=1.83 Å) determined averaging the data of all the neptunium(V) structures referenced in the Cambridge

database.[70] The equatorial plane distances are in the range 2.496(2)-2.516(2) Å and 2.706-2.712(2) for the carbonyl and ether groups respectively. These distances are quite longer compared to other actinyl(VI) diglycolamide structures (U(VI)-TEDGA[71,72] and Pu(VI)-TMDGA[73]). A similar structure with Np(V) was already described by Tian et al. with the TMDGA (TetraMethylDiGlycolAmide) ligand[74] and presents similar distances compared to the actinyl(VI) solids. The average An-$O_{carbonyl}$ and An-O_{ether} bonds for these literature structures are 2.42 Å and 2.60 Å respectively. The oxidation state of the Np(V)-TMDGA structure is reported to be +V by the authors[74], but (i) the yl bond length of 1,73 Å, (ii) the distances of the coordination sphere similar to those of the other actinyl(VI) structures and (iii) the bond valence calculation in the range 6.18 or 6.34 depending on parameters used for Np–O bonds[15,68,69] seem to suggest that the real oxidation state of the previously described Np(V)-TMDGA structure is +VI. The lengthening of the coordination distances for our Np(V) structure compared to the literature An(VI) structures is thus consistent with the charge modification between the two oxidation states. Our neptunium compound (**3**) is thus the first An(V)-diglycolamide structure reported in the literature. With an average of 1.24(1) Å and 1.33(1) Å respectively, the C=O and C-N distances are in agreement with TEDGA structures reported in the literature with actinyl[71,72] or lanthanide(III)[75,76]. The charge compensation is ensured by one interspace nitrate ion, and two water molecules taking part to the hydrogen bond network are also present around the Np(V) monomer.

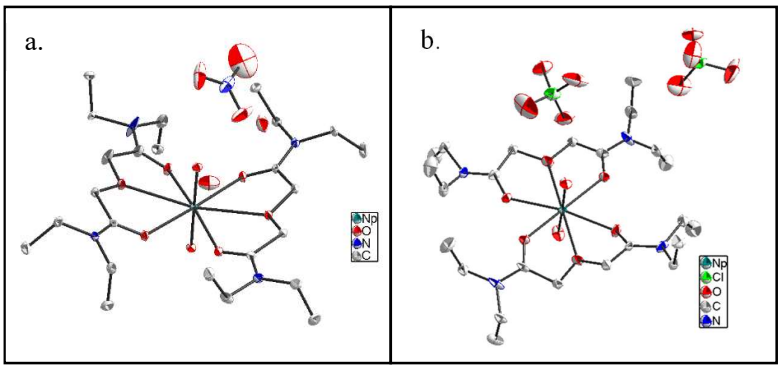

Figure 1: Structures of (a.) $[Np^{V}O_2(TEDGA)_2].NO_3.2H_2O$ (**3**) and (b.) $[Np^{VI}O_2(TEDGA)_2].2ClO_4$ (**4**)

The Np(VI)-TEDGA monomer (**4**), $[Np^{VI}O_2(TEDGA)_2].2ClO_4$, was described in the monoclinic system with C2 space group. The yl distances of 1.748 Å, very close to the one of the Np(VI)-TEDGA-triflate structure[77], indicates the +VI oxidation state for the neptunium in the structure. The BVS calculations (see table 2) between 6.11 and 6.25 are in agreement with the oxidation state expected from the yl distances. This structure is nearly identical to the Np(V) monomer (**3**) with two tridentate TEDGA ligands in the equatorial plane. The comparison with the other actinyl structures shows very similar An-$O_{carbonyl}$ bond distances with 2.420(1) Å and 2.415(1) Å for compound (**4**) and average of literature structures respectively.[71,72,73,74] Nevertheless, the An-O_{ether} distances with 2.618(1) Å for (**4**), in

agreement with the Np(VI)-TEDGA-triflate structure, 2.61(8) Å,[77] are significantly longer than the 2.596(1) Å reported for the An(VI) structures.[71,72,73,74]

Table 2: Bond valence sum (BVS) values of the neptunium atoms for structures **1**, **2**, **3**, **4** and Np-TMDGA structure (see SI for more details - SI-XRD-UV-DFT file).

Reference of the parameter		68	69	15
Trimer (**1**)	Np1	4.96	4.96	4.92
	Np2	5.77	5.75	5.82
Dimer (**2**)	Np1	4.95	4.96	4.91
	Np2	6.03	6.02	6.07
Np(V)-TEDGA (**3**)		5.03	5.03	5.02
Np-TMDGA[74]		6.21	6.18	6.34
Np(VI)-TEDGA (**4**)		6.14	6.11	6.25

Trimer structural description - The trimer (**1**), $[Np^{V}O_2(TEDGA)_2]_2.[Np^{VI}O_2(NO_3)_2].(NO_3)_2$, crystallizes in the triclinic space group P-1. The molecular structure of the trimer presented in Figure 2 consists of a mixed-valence compound based on one central Np(VI) (Np_2^{VI}) linked to two lateral Np(V) (Np_1^{V}) atoms via CCIs, i.e. via the oxo groups of the pentavalent neptunium. The two Np(V) are crystallographically equivalent due to an inversion center located on the Np(VI) and the three actinides are thus perfectly aligned with an angle of 180° while the $Np_1{=}O\cdots Np_2$ angle is 175.61(1)°. The yl distances of the free oxo $Np_1^{V}{=}O_{free}$, 1.806(1) Å, are in the range of the monomer (**3**) and the literature ones. [70] The oxo groups involved in the CCIs present a longer yl bond $Np_1^{V}{=}O_{CCI}$ of 1.864(1) Å because of the electronic delocalization toward the central Np(VI) atom. This distance is in agreement with the Np(V) involved in CCIs distances reported in the literature, 1.81-1.91 Å[19,78]. The hexavalent neptunium presents a $Np_2^{VI}{=}O$ yl bond of 1.780(1) Å which is close to the 1.720-1.785 Å range reported in the literature,[70] and longer than the yl bond (1.720(1) Å[56]) of the dinitrate Np(VI) monomeric structure, $Np^{VI}O_2(NO_3)_2(H_2O)_2$, that differs only by the presence of water molecules instead of the Np(V) oxo groups, showing the impact of the yl interaction on the CCI-acceptor. The angles of the yl moieties are 178.2° and 180° (inversion center) for Np_1^{V} and Np_2^{VI} respectively, in agreement with the awaited linearity. The distance between the two actinide centers is 4.183(2) Å.

In order to confirm the oxidation state of the neptunium in the trimer, the bond valence model was applied[65] (table 2) based on different parameters reported for Np–O bonds.[15,68,69] The values for neptunium atoms are consistent with a localized valence of +5 and +6 for the pentavalent state Np_1^{V} and hexavalent state Np_2^{VI} respectively. This BVS analysis supports the formation of a mixed Np(V)-Np(VI) trimer. The Np(V) is the oxidation state which is sharing its oxo ions as the yl bond of a hexavalent neptunium is stronger (Lewis basicity) than the Np(V) one. The Np(VI) yl bond is thus relatively inert and rarely engaged in intermolecular interactions.[16]

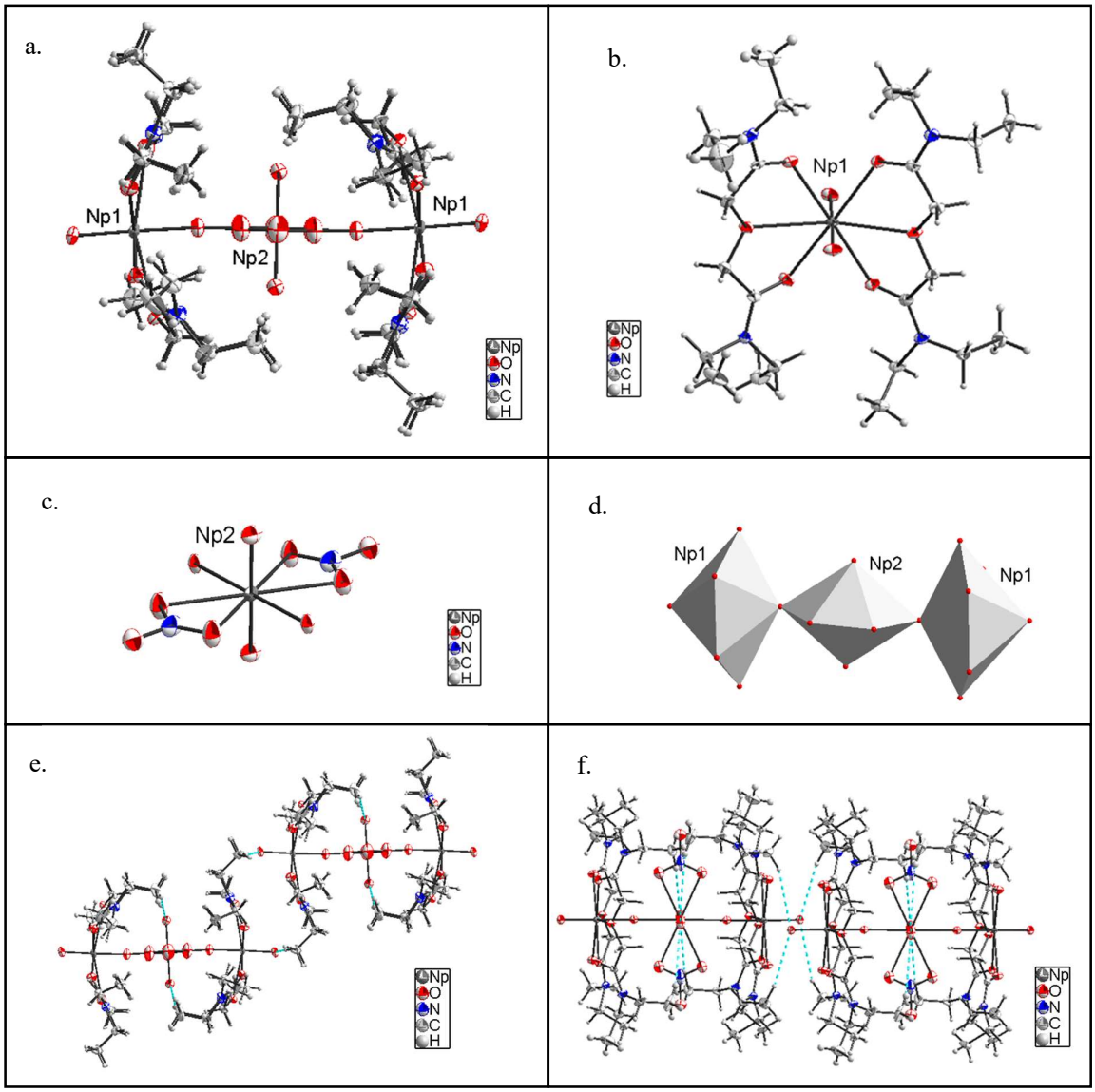

Figure 2 – Structure of the Np(V)-Np(VI) trimer (**1**), $[Np^{V}O_2(TEDGA)_2]_2.[Np^{VI}O_2(NO_3)_2].(NO_3)_2$: (a) View of the trimer, (b) coordination sphere of the Np_1^{V} atom, (c) coordination sphere of the Np_2^{VI} atom, (d) polyhedral view showing the alignment of the trimer, (e) lateral view allowing the observation of the TEDGA ligands orientation and (f) packing of the trimer units highlighting the short distances between the trimers. The hydrogen bonds are in cyan color.

In addition of the two oxo groups from their neighboring Np_1^{V}, two bidentate nitrate anions complete the coordination sphere of the central Np_2^{VI} (Figure 2c). The oxygen atoms of the two nitrates are located at distances from the metallic cation of 2.580(1) and 2.577(1) Å which is consistent even if longer than the Np^{VI}-O distances of the Np(VI) nitrate structure,[56] with an average bond of 2.50(1) Å. The oxygen

atoms of the Np_1^V oxo group is at a distance of 2.322(1) Å from Np_2^{VI}, which is typical for an equatorial oxygen atom engaged in a cation-cation interaction[15,79] but shorter than the Np^{VI}-O_{water} average distances of 2.43(1) of the Np(VI) nitrate structure.[56] This shorter Np_2^{VI}-O_{CCI} distance associated to the longer Np(VI) yl bond of the trimer, 1.780(1) Å compared to the nitrate structure, 1.752(1) Å as well as the longer distances of the nitrate oxygen atoms reveal the strong interaction of the Np(V) oxo group in the Np(VI) equatorial plane.

The Np_1^V equatorial plane is composed of two tridentate TEDGA ligands that are connected through the two carbonyl functions and the central ether group as for the monomeric structure (**3**) (see Figure 2b). The Np_1^V-$O_{carbonyl}$ distances are in the range 2.474(1)-2.543(1) Å with an average of 2.51(1) Å, i.e. similar to the monomer ones (**3**) with 2.51(1) Å. This is also the case for the ether oxygen with an average Np_1^V-O_{ether} distance of 2.68 Å for the Np(V)-Np(VI) trimer (**1**) and 2.71 Å for the monomer (**3**). Nevertheless, even if the distances average corresponds to the literature, the two TEDGA molecules do not interact identically with the Np_1^V as quite different Np_1^V-O_{ether} and Np_1^V-$O_{carbonyl}$ distances are observed for the two non-crystallographycally equivalent TEDGA. One TEDGA presents a Np_1^V-$O_{carbonyl}$ distance of 2.481(1) Å and a Np_1^V-O_{ether} bound of 2.738(1) Å whereas the other one has Np_1^V-$O_{carbonyl}$ distance of 2.533(1) Å and a Np_1^V-O_{ether} distance of 2.615(1) Å. The shortening of the amide oxygen atom induces the significant longer distance of the ether group. These differences between the two TEDGA atoms are likely due to long-range interactions.

Indeed, the TEDGA molecules present a surprising orientation within the trimer (see figure 2e). Contrary to the monomers (**3** and **4**), the TEDGA molecules do not adopt a symmetrical geometry around the cation. The angle between the two planes formed by the O atoms of each TEDGA is 46(1)° in the CCI structure against 23(1)° for the monomer structures. However, the weak evolution of the O-C-C-O torsion angles within the ligand indicates that the TEDGA is quite rigid and the changes come from a global orientation of the molecules in relation to the equatorial plane. According to figure 2e, the TEDGA with shorter An-O distances but longer ether ones bent unexpectedly toward the yl of the central neptunium. One can await the opposite because of steric constraints. Nevertheless, weak intermolecular interactions (H bonds beyond the Van der Walls limit[80]) between the alkyl chains and the central yl are likely the origin of this tendency. This TEDGA orientation allows an extremely close packing of the trimers with the yl of the Np_1^V of the first trimer unit located between the alkyl chains of the TEDGA of a second trimer; this arrangement gives a distance between the two Np_1^V equatorial planes from adjacent trimers in the 2.503-2.549 Å range. These extremely short distances are possible thanks to an offset between the two trimers so the yl bonds are not aligned. This packing enables the establishment of other intermolecular H bonds (figure 2f) between the ethyl chains and the nitrate ions on the one hand and the oxo group of the neighboring trimers on the other hand.

Dimer structural description – The dimer (**2**) is close to the mixed-valence trimer arrangement of **1** with the Np_2^{VI} linked to the Np_1^{V} atoms via CCIs, i.e. via the oxo groups of the pentavalent neptunium with a distance of 2.281(1) Å (figure 3a). The bond valence calculations validate the oxidation states of the two neptunium atoms. The trans di-oxo groups of Np_1^{V} are nearly aligned (angle of 179.8°) and the distances are 1.805 and 1.881(1) Å, with the longer one for the oxygen atom involved in the CCI. This last bond longer in the dimer (**2**) than in the trimer (**1**), as well as the shorter CCI distance, $Np^{V}=O_{yl}.\cdots Np^{VI}$, of 2.281 (1) Å, likely indicates a stronger interaction in the dimer structure (**2**) than in the trimer (**1**) one. The coordination sphere of the Np_1^{V} is composed of two TEDGA molecules with distances from the Np(V) shorter by 0.018 Å compared to the trimer (**1**) ones (see figure 3b). It is connected to the stronger charge transfer of the CCI in the dimer. The peculiarity of the Np(VI) atoms does not lie in the Np_2^{VI}=O bonds of 1.769(1) and 1.765(1) Å but in its angle of 169.9° that is significantly removed from linearity. This feature is related to the presence of three bidentate nitrates in the coordination sphere in addition to the O atom from the CCI (see figure 3c). To accept this coordination number of 7, one of the nitrate ion is perpendicular to the equatorial plane inducing the bending of the yl moiety. One oxygen of this particular nitrate is quite far from the central metallic cation with a distance of 2.746(1) Å. The other $O_{nitrate}$-Np_2^{VI} distances are between 2.519- 2.584(1) Å which is in agreement with the structures referenced in the CCDC[70] with Np(VI)-O distances ranging between 2.363 and 2.651 Å (CN=6). The length of the furthest nitrate is thus out of the normal range. The CN of 7 has already been reported for actinyl coordination sphere containing nitrate ions with seven uranyl structures described in the literature[81,82,83,84]. The asymmetry of the perpendicular nitrate is not singular either and was already observed for 5 out of the 7 uranyl structures. The An-O_{long} of this specific perpendicular nitrate is 6 to 14% longer than the An-O_{short} for these structures and in the same order of magnitude as the one of the present dimer (**2**) with 6%. The angle of the O=U=O moiety varies from 166.2 to 174.7°. With 169.9, the neptunyl angle of Np_2^{VI} is within this range.

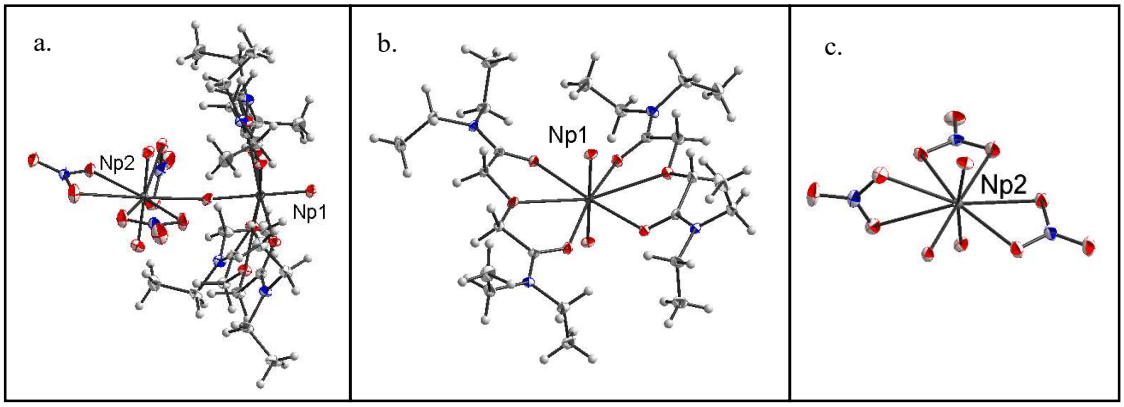

Figure 3 – Structure of the Np^{V}-Np^{VI} dimer (**2**), $[Np^{V}O_2(TEDGA)_2].[Np^{VI}O_2(NO_3)_3].ACN$: (a) View of the dimer, (b) coordination sphere of the Np_1^{V} atom, (c) coordination sphere of the Np_2^{VI} atom.

The dimer presents the same TEDGA orientation as the trimer with the TEDGA bending towards the Np(VI) clearly indicating that the interactions are not driven by steric constraint. The same large angle of 48° between the two planes formed by each TEDGA oxygen atoms is observed.

DFT calculations

The geometries of $[Np^{V}O_2(TEDGA)_2]^{+}$ **(3)**, $[Np^{V}O_2(TEDGA)_2][Np^{VI}O_2(NO_3)_3]$ **(2)** and $[Np^{V}O_2(TEDGA)_2]_2[Np^{VI}O_2(NO_3)_2]^{2+}$ **(1)** were optimized starting from their crystal structures. The structures are shown in Figure 4 and the main structural parameters are listed in Table 3.

Table 3. Selected geometric parameters and Np atomic charges from DFT calculations for monomer **(1),** dimer **(2),** trimer $[NpO_2(TEDGA)_2]_2[NpO_2(NO_3)_2]^{2+}$ **(3)**, and $Np^{VI}O_2(NO_3)_2(H_2O)_2$. Calculated distances are compared to XRD experimental values. B3LYP-D3/6-31+G(d,p) calculations in the gas phase. Np atomic charges are derived from an AIM analysis.

	Monomer **(3)**		Dimer **(2)**		Trimer **(1)**		$NpO_2(NO_3)_2(H_2O)_2$	
	Calc.	XRD	Calc.	XRD	Calc.	XRD	Calc.	XRD[56]
Distances in Å*								
Np^{VI}-O_L	-	-	2.371	2.281	2.315	2.323	2.528	2.438
L=Np, H_2O								
Np^{VI}-O_{nit1}	-	-	2.552	2.538	2.575	2.580	2.477	2.507
Np^{VI}-O_{nit2}	-	-	2.482	2.528	2.575	2.580	2.477	2.507
Np^{VI}-O_{nit3}	-	-	2.470-3.542	2.583-2.746	-	-		
Np^{VI}=O_{yl}	-		1.762	1.767	1.767	1.782	1.746	1.747
Np^{V}=O_{1yl}	1.803	1.804	1.876	1.881	1.890	1.864	-	-
Np^{V}=O_{2yl}	1.803	1.838	1.785	1.805	1.788	1.808	-	-
Np^{V}-$O_{carbonyl1}$	2.576	2.514	2.503	2.479	2.484	2.481	-	-
Np^{V}-O_{ether1}	2.830	2.707	2.877	2.715	2.760	2.615	-	-
Np^{V}-$O_{carbonyl2}$	2.588	2.504	2.569	2.505	2.491	2.533	-	-
Np^{V}-O_{ether2}	2.830	2.713	2.696	2.639	2.829	2.739	-	-
Angles*								
O_{yl}=Np^{VI}=O_{yl}	180°	179°	177°	170°	180°	180°		
O_{yl}=Np^{V}=O_{yl}	-	-	180°	180°	179°	178°	180°	180°
Np^{VI}··· O_{1yl}=Np^{V}	-	-	176°	173°	162°	175°	-	-
O_{ether1}··· Np^{V}=O_{1yl}	76°	81°	73°	75°	80°	79°	-	-
O_{ether2}··· Np^{V}=O_{1yl}	104°	85°	85°	82°	100°	79°	-	-
AIM charges								
q(Np^{V})	2.576	-	2.645	-	2.650	-	-	-
q(Np^{VI})	-	-	2.821	-	2.824	-	2.853	-

* In dimer and trimer structures, O_{1yl} denotes the oxygen atom from NpO_2^{+} involved in the cation-cation interaction, while O_{2yl} is the second NpO_2^{+} oxygen atom, which remains unbound.

*Monomer structure **(3)**.* As depicted in Figure 4, the calculated and XRD structures differ in the relative arrangement of the TEDGA molecules around Np(V). In the crystal structure, the nitrogen and ether oxygen atoms (O_{ether}) of the two TEDGA molecules are out of the equatorial plane and point in the same direction (see the representation of the TEDGA molecule figure S1 in the SI). However, in the optimized structures these atoms point in opposite directions, as indicated by the values of the angle between ether oxygen atoms and one Np^{V}=O_{yl} bond (O_{ether}··· Np^{V}=O_{1yl} angle in table 1), the angles are below 90° in

the crystal structures, whereas in the calculated structure they are both above and below 90°. The relative orientation of the two TEDGA ligands can be influenced by external interactions, such as crystal packing force or solvent effect in solution. This is demonstrated by the geometry optimizations of $[Np^{V}O_2(TEDGA)_2]^+$ in the presence of a continuum solvent model (see Table S2 in SI section - SI-XRD-UV-DFT file); oxygen and nitrogen atoms of the two TEDGA become nearly coplanar and all belong to the neptunyl equatorial plane.

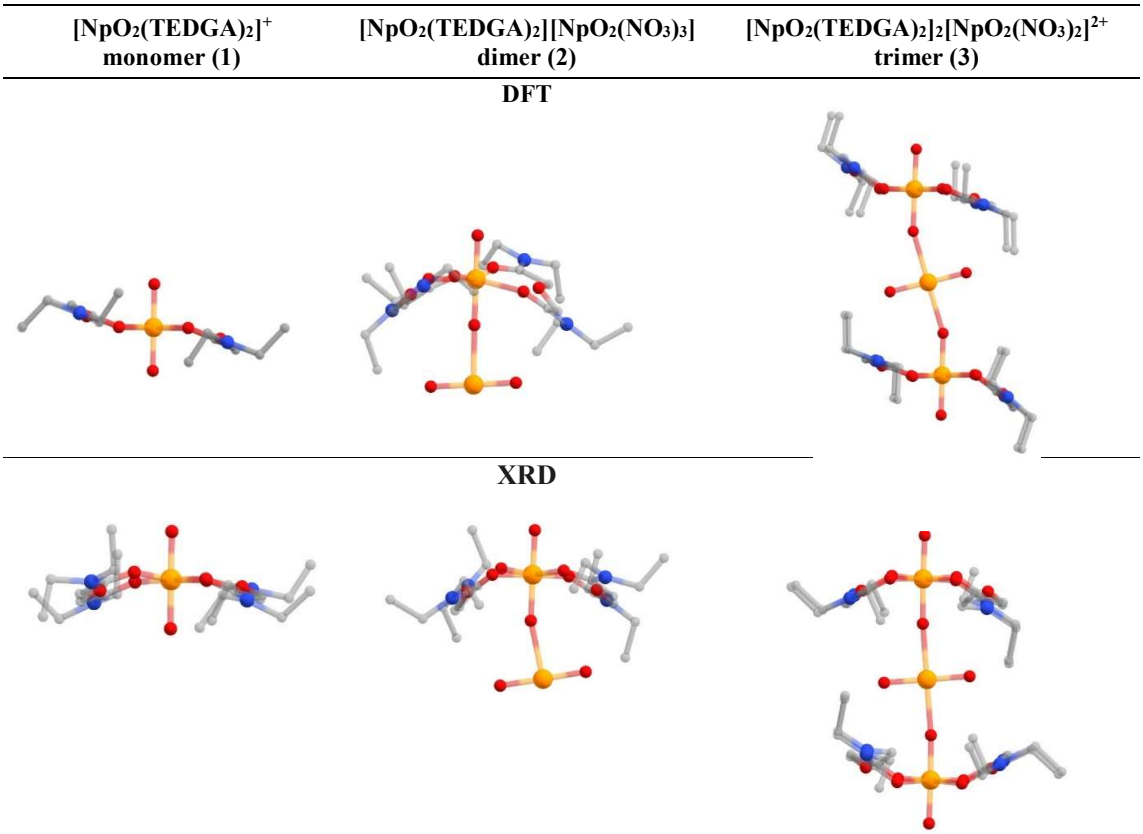

Figure 4. Relative orientation of TEDGA ligands around $Np^{VI}O_2^+$ in the monomer **(1)**, dimer **(2)** and trimer **(3).** Top : DFT calculations, Bottom : XRD. Hydrogen atoms and nitrate ions are omitted for clarity.

*Trimer structure **(1)***. As found in the monomer structure, the relative orientation of TEDGA differ between the XRD and calculated structure (Figure 4). Some deviations are also found in the relative arrangement of the three neptunyl units ("T-Shape" structure). In the crystal structures for the trimeric species, the three neptunyl units are nearly linearly arranged with a $Np^{V}=O_{yl}.\cdots Np^{VI}$ angle equal to 175°, whereas in the calculated structure it is slightly bent at 162°.

The calculated Np-O bond distances are in correct agreement with the XRD values. The trimer $Np^{V}=O_{yl}.\cdots Np^{VI}$ cation-cation distance (Np^{VI}-O_L in table 3) is particularly well reproduced in the

calculations. It should be mentioned that it is only by introducing dispersion corrections using the D3 correction method of Grimme[61,62] in the DFT/B3LYP calculations that it is possible to reproduce correctly the cation-cation distance. The B3LYP results without dispersion corrections are given in the SI section (Table S3 - SI-XRD-UV-DFT file). The $Np^{V}=O_{yl}.\cdots Np^{VI}$ cation-cation distances (Np^{VI}-O_L in table 3) are ~0.06 Å longer in the absence of dispersion model while other bond distances are not strongly influenced. This indicates the key role of weak interactions in the CCIs.

In order to better understand the interactions governing the cation-cation structure and stability, DFT calculations were done on model trimeric structures by varying the TEDGA ligand bound to Np(V) and the counter-ion bound to Np(VI). The TEDGA ligand was substituted with TMDGA (TetraMethylDiGlycolAmide) and nitrate ions were replaced with chloride ions. This results in $[NpO_2(DGA)_2]_2[NpO_2(NO_3)_2]^{2+}$ and $[NpO_2(DGA)_2]_2[NpO_2(Cl)_2]^{2+}$ with DGA=TMDGA or TEDGA. As shown in Figure 5, changing the DGA ligand as well as the counter anion influences the trimeric structure. This shows the existence of multiple low-energy conformations associated with various relative arrangements of neptunyl and diglycolamide. With chloride anions, the relative arrangement of the DGA ligands differs from that calculated with nitrate ions but is similar to the one obtained in the trimeric XRD structure (with nitrate ions). With TMDGA, the most stable structure corresponds to three linearly arranged neptunyl units, resembling the trimer XRD structure whereas it is bent with TEDGA. DFT calculations were reported for the T-shaped neptunyl-neptunyl (with $Np(V)O_2^+$ units)[85] and neptunyl-uranyl dimeric units.[86] "Bent" T-shaped structures were found for hydrated and nitrate dimer species and were attributed to hydrogen-bonding interactions occurring between water ligand and O_{yl}. There is no water ligand in the present trimeric species, but weak interactions involving DGA alkyl groups, counter ions and O_{yl} may have such influence. The cation-cation binding energies were calculated between the core unit $Np^{VI}O_2(A)_2$ ($A=NO_3^-$ or Cl^-) and the two $Np^{V}O_2(DGA)_2^+$ units (DGA=TEDGA or TMDGA). Energy variations (ΔE in $kJ.mol^{-1}$) are given in Figure 5. Replacing nitrate by chloride anions increases the binding strength by 14 $kcal.mol^{-1}$ with both TMDGA and TEDGA ligands. This is associated with a diminution of the cation-cation distance (Np^{VI}-O_{Np}) between neptunyl oxygen atoms by 0.07-0.08 Å. This is expected due the higher electronic charge on Np(VI) atom with chloride ions inducing stronger cation-cation interactions, as well as the reduced steric hindrance effects in the Np(VI) coordination sphere, the coordination number decreasing from six with nitrate ions to four with chloride ions. Replacing TEDGA by TMDGA also increases the cation-cation binding strength by 9 $kcal.mol^{-1}$ for both anions but this is not associated with a diminution of the cation-cation distance, which increases slightly. The energy difference is not due to an electronic donor effect from ethyl groups, TEDGA ethyl groups do not increase the oxygen electronic charge on neptunyl compare to TMDGA. Weak interactions involving the DGA alkyl groups and oxygen or chloride atoms from $Np^{VI}O_2(A)_2$ can induce such energy difference, as illustrated by the strong influence of dispersion corrections in the calculated binding energy (Table S4 - SI-XRD-UV-DFT file). Of course, in the solid state or in solution, other intermolecular interactions may counterbalance these forces within the trimer

and influence its structure and stability. However, these results support the key role of weak interactions in such system.

$[NpO_2(\mathbf{TMDGA})_2]_2[NpO_2(\mathbf{NO_3})_2]^{2+}$	$[NpO_2(\mathbf{TMDGA})_2]_2[NpO_2(\mathbf{Cl})_2]^{2+}$
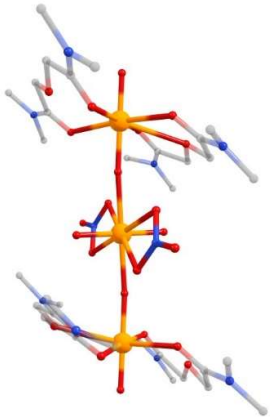	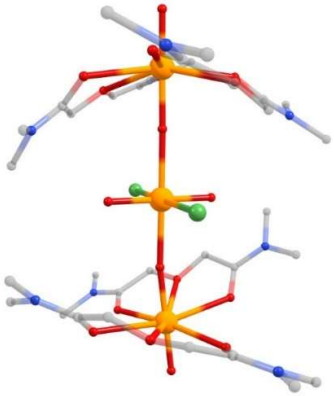
Np^{VI}-O_{Np} =2.313Å Np^{V}=O_{yl}-Np^{VI}=171° ΔE=-71 kcal.mol^{-1}	Np^{VI}-O_{Np} =2.248Å Np^{V}=O_{yl}-Np^{VI}=175° ΔE=-85 kcal.mol^{-1}
$[NpO_2(\mathbf{TEDGA})_2]_2[NpO_2(\mathbf{NO_3})_2]^{2+}$	$[NpO_2(\mathbf{TEDGA})_2]_2[NpO_2(\mathbf{Cl})_2]^{2+}$
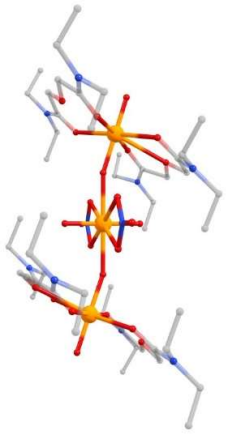	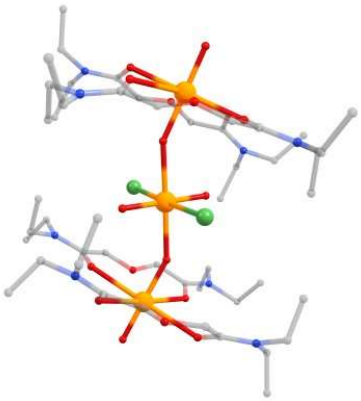
Np^{VI}-O_{Np} =2.315Å Np^{V}=O_{yl}-Np^{VI}=162° ΔE=-80 kcal.mol^{-1}	Np^{VI}-O_{Np} =2.262 Å Np^{V}=O_{yl}-Np^{VI}=152° ΔE=-94 kcal.mol^{-1}

Figure 5. DFT calculations for $[NpO_2(DGA)_2]_2[NpO_2(A)_2]^{2+}$ trimers, with A=NO_3^- or Cl^- and DGA=TMDGA or TEDGA). Optimized structures and binding energies (energy variations ΔE in kJ.mol^{-1}) corresponding to the binding energies between $Np^{VI}O_2(A)_2$ and two $Np^{V}O_2(DGA)_2^+$ units. B3LYP-D3/6-31+G(d,p) calculations in the gas phase.

*Dimer Structure **(2)***. The relative orientation of TEDGA is well reproduced in the calculated dimer structure, however the bidentate coordination mode of the three nitrate ions is not. The peculiar bidentate nitrate observed in the XRD structure turns to a monodentate coordination mode, resulting in a

coordination of six for the neptunium(VI) instead of seven. The longer Np(VI) oxygen nitrate distance is measured at 2.75 Å but calculated to be 3.54 Å. As a result, the nitrate oxygen atom is no longer bound to the neptunium atom in the calculations. The calculated Np^{VI}-O_{nit} distances for the remaining coordinated oxygen atoms is shorter (2.482 Å) than the measured value (2.583 Å). The incorrect reproduction of the nitrate coordination modes may indicate that intermolecular or packing interactions are responsible for the specific coordination mode in the crystal structure. The neptunyl angle is no longer distorted in the calculation and is nearly linear with 177°. The calculated structure is closer to the ideal T-Shape structure with an Np^{V}=O_{yl}.⋯ Np^{VI} angle of 176°, while it is slightly bent in the XRD structure (173°).

Vibrational spectroscopy

The vibrational spectra of the Np(V)-Np(VI) trimer (**1**) and dimer (**2**) are presented figure 5 and compared to those of the Np(V)-TEDGA (**3**) and Np(VI)-TEDGA monomers (**4**), the free TEDGA and the Np(VI) di-nitrate structure.[56] The spectrum of the Np(VI) dinitrate structure[56] exhibits a large, intense band above 1200 cm^{-1}, characteristic of a fluorescence phenomenon frequently observed in Raman spectroscopy. Nevertheless, the yl and main nitrate features can be discussed. Vibrational frequencies were also calculated using DFT for all the species. The band attributions, based on these calculations and the literature,[87, 88, 89, 90, 91, 92, 93, 94, 95] are presented in table 5 for the TEDGA ligand and the counter ion (nitrate or perchlorate) and in table 6 for the yl attribution.

TEDGA and counter ion band attribution

The C=O stretching of the free ligand is observed between 1643-1663 cm^{-1}. The bands centered at 1484 and 1455 cm^{-1} are attributed to $\nu_{out\ of\ phase}$C=O and O=C−CH_2−O coupled to ν C=O, whereas the ones at 1292 and 1265 cm^{-1} are assigned to ν O=C-N and wagging of the CH_2 groups. The very large band at 1080 cm^{-1} gathers two vibrational modes: asymmetric stretching of the ether function and twisting of the CH_2. The symmetric stretching of the ether is observed at 801 cm^{-1}. The bands below 700 cm^{-1} are attributed to the deformation of the N-C=O moiety. With complexation, for either the trimer (**1**), dimer (**2**) or the monomer (**3**), there is a shift of the C=O, O=C-N and ether bands that is similar for the three structures. The bands corresponding to the alkyl chains also evolved with complexation and the shift depends on the structure likely related to the nature of the counter ions and the various intermolecular interactions. The Np(VI)-TEDGA (**4**) monomer complex reduces under the Raman beam as the time or the laser power increase. To collect the signal of the complex and not its reductive contribution, the acquisition was done with a short acquisition time and with a laser power of 0.3mW making difficult to observe the less intense bands. As a result, only a few bands of TEDGA are visible in the spectrum, especially those at 771 cm^{-1}, 1640 cm^{-1} and within the 1451-1521 cm^{-1} range.

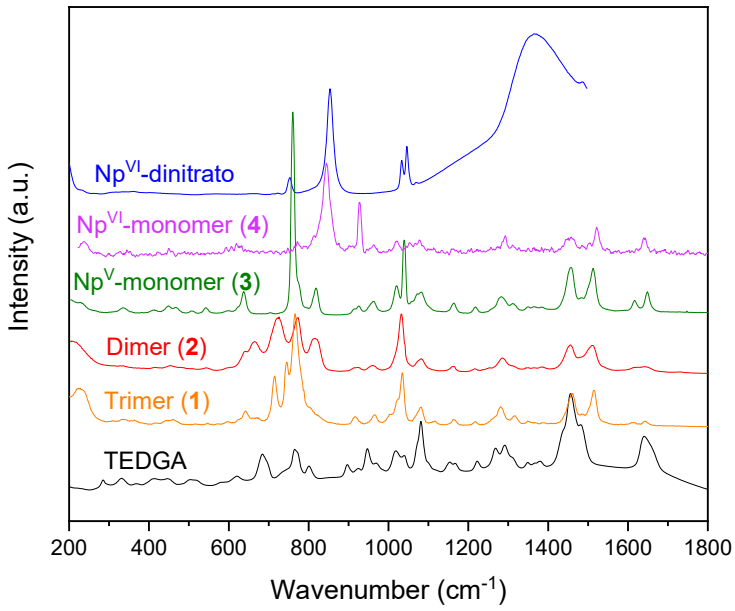

Figure 5 – Raman spectra of the Np(V)-Np(VI) trimer (**1**) and dimer (**2**) compared to those of Np(V) monomer (**3**), Np(VI) monomer (**4**) (plotted with a multiplicative factor of 15), the free TEDGA and the Np(VI) di-nitrate structure[56].

The coordinated nitrate symmetric stretchings for structures (**1**) and (**2**) appear at 1034 and 1031 cm^{-1} respectively, and at 1046 and 1033 cm^{-1} for the dinitrate Np(VI) structure. The broadness of the band for the polynuclear species indicates the presence of several nitrate contributions: free nitrates and coordinated ones for the trimer (**1**) and bidentate and asymmetric bidentate groups for the dimer (**2**). The decrease of the wavenumber from dinitrate structure towards the trimer or dimer is consistent with the cation – cation interactions with the neptunium(V) oxo bond in (**1**) or (**2**) stronger than the water molecules one in the dinitrate structure. It is also in agreement with the variation of Np(VI)-O distances discussed earlier. The charge compensation in the monomer **3** is ensured by free nitrate ions, whose main bands are observed at 1042 cm^{-1}. The other Raman active bands around 720 and 1450 cm^{-1} corresponding to the bending of the nitrate are probably superimposed with the TEDGA signals in this wavenumber range.

The counter ions of the Np(VI) monomer (**4**) are perchlorate. Due the data collection conditions, only two out of the four bands of the perchlorate ions can be attributed: the symmetric bending mode (v1) at 927 cm^{-1} and the asymmetric stretching vibration at 1079 cm^{-1}.[96]

Table 5 – Raman band attribution (in cm^{-1}) for the TEDGA ligands and counter ions of the Np(V)-Np(VI) trimer (**1**) and dimer (**2**), the Np(V) monomer (**3**), the free TEDGA and the Np(VI) nitrate structures. (l= large, sh=shoulder).

	Free TEDGA	Np trimer (**1**)	Np dimer (**2**)	Np^{V}-monomer (**3**)	Np^{VI}-monomer (**4**)	$Np^{VI}O_2(NO_3)_2(H_2O)_2$ [56]
$\nu_{in\ phase}$ C=O TEDGA	1646 (l)	1645 1612	1648 1618	1649 1616	1640	-
$\nu_{out\ of\ phase}$ C=O O=C−CH_2−O coupled to ν C=O And $\nu_{3\ as}$ NO_3	1484 (l) 1455 (l)	1513 1457	1511 1458	1511 1455	1521 1451	-
$\nu_{4\ in\ plane}$ NO_3 ν O=C-N TEDGA ν CH_2 wagging TEDGA	Several bands between 1311-1265	Several bands between 1316-1281	Several bands between 1315-1288	Several bands between 1312-1280	-	-
ν CH_2 twisting TEDGA ν_{as} CH_2-O-CH_2 TEDGA	1082 (l)	1081(l)	1083(l)	1083(l)	-	-
ν_3 ClO_4	-	-	-	-	1079	-
ν_{1s} NO_3	-	1034	1031	1042	-	1046 1033
ρCH_2 et alkyl?	1018	1021	1018	1020	1020	-
ρCH_2	946-968	964	962	960	963	-
ν_1 ClO_4	-	-	-	-	927	-
νs CH_2-O-CH_2 TEDGA	801	790-820 (l)	810 (l)	818	820	-
Alkyl chains TEDGA	766-773	764	773	774 (sh)	771	-
ν_6 NO_3	-	744	724 (l)	Too small	Too small	752
Def N-C=O	682 696	641	664 640	637	630	-

Neptunyl band attribution

The attribution of the neptunyl Raman bands for the monomers are straight as the vibrational band corresponding to the ν_1 stretching mode is particularly intense. The Np(V) ν_1 stretching band in the Np(V)-TEDGA complex (**3**) is attributed at 760 cm^{-1} where as the one of the Np(VI) in the Np(VI)-TEDGA compound (**4**) is at 846 cm^{-1}.

The attribution of neptunyl vibration modes in the CCI structures is not straightforward. Indeed, it is no longer possible to consider the Np(V) and Np(VI) yl separately; extended neptunyl-neptunyl interactions lead to vibrational modes involving combinations of the ν_1 (symmetric) and ν_3 (asymmetric, normally forbidden in Raman spectroscopy[78,98]) of Np(VI)-yl and Np(V)-yl moieties. All the modes are Raman active. Such combinations were previously reported in a recent experimental and computational study on model Np(V) dimers et trimers by Pyrch *et al.*.[85] To aid in band assignment, vibrational frequencies were calculated using DFT for the monomer, dimer and trimer species. The calculated vibrational

frequencies systematically deviate from experimental values due to the neglect of anharmonic effects and calculation errors inherent to the choice of methodology. To account for these discrepancies, a scaling factor λ was applied. This factor was determined by matching the calculated neptunyl frequency in $Np^{V}O_2(TEDGA)_2^+$ (**3**) at 808 cm^{-1} with the experimentally measured value of 760 cm^{-1} (λ = 0.9406). The corrected vibrational frequencies calculated for the neptunyl vibrations in the 750-900 cm^{-1} region are given in Table 6. It should be noted that the calculations do not take into account the intermolecular interactions in trimers (**1**), specifically between the alkyl chains of the amide groups and the Np(VI)-yl moiety and that they fail to preserve the coordination number of seven for dimer (**2**) during geometry optimization. Despite these limitations, they still offer a reliable estimates of the expected range for the Np(VI)-yl symmetric stretching vibration. For the dimer (**2**), an intense Raman active neptunyl vibration mode is calculated at 815 cm^{-1}. In the experimental spectrum, this band is likely superimposed with the ν_{sym} CH_2-O-CH_2 of the TEDGA ligand forming a large band with a shoulder centered at 816 cm^{-1}. For the trimer (**1**), two Raman-active vibrational modes are calculated at 687 and 816 cm^{-1}. They correspond to a combination of $\nu_1(NpO_2^+)$-$\nu_1(NpO_2^{2+})$ and $\nu_3(NpO_2^+)$-$\nu_1(NpO_2^{2+})$ respectively. These modes can be attributed to the two bands at 715 cm^{-1} and 805 cm^{-1} contained in the experimental spectrum. The 805 cm^{-1} band appears at the base of the alkyl chains signal. These values of CCI neptunyl vibrations are in good agreement with those reported in the literature for CCI compounds.[9, 78,97,98,99,100]

Table 6. Calculated vibrational modes and Raman activities involving the Np^{VI} and Np^{V} neptunyl stretching vibrations for monomers **(3** and **4)**, dimer **(2)**,trimer **(1)** and $NpO_2(NO_3)_2(H_2O)_2$.. B3LYP/6-31+G(d,p) calculations in the gas phase.

	Theoretical Frequency (cm^{-1})	Theoretical Raman activity ($Å^4$/amu)	Theoretical Frequency scaled values* (cm^{-1})	Experimental frequencies	Assignment
Trimer (**1**)	730	389	687	715	ν_1 NpO_2^+, ν_1 NpO_2^{2+}
	844	4	794	-	ν_1 NpO_2^+, ν_1 NpO_2^{2+}
	849	0	799	-	ν_3 NpO_2^+
	867	117	816	805 (sh)	ν_3 NpO_2^+, ν_1 NpO_2^{2+}
	939	0	883	-	ν_3 NpO_2^{2+}
Dimer (**2**)	852	48	801	-	ν_1 NpO_2^+, ν_1 NpO_2^{2+}
	866	110	815	823 (sh)	ν_3 NpO_2^+, ν_1 NpO_2^{2+}
	945	1	889	-	ν_3 NpO_2^{2+}
Np(V)-Monomer	808	39	760	760	ν_1 NpO_2^+
(**3**)	878	0	826	-	ν_3 NpO_2^+
Np(VI)-Monomer			0	846	ν_1 NpO_2^{2+}
(**4**)		0	0	-	ν_3 NpO_2^{2+}
$NpO_2(NO_3)_2(H_2O)_2$ [56]	892	102	839	852	ν_1 NpO_2^{2+}
	988	0	929	-	ν_3 NpO_2^{2+}

* Scaling factor λ=0.9406

Conclusions

Herein, we described two new mixed valence Np(V)-Np(VI) cation-cation interaction compounds that were stabilized with TEDGA ligand: one trimer, $[Np^{V}O_2(TEDGA)_2]_2[Np^{VI}O_2(NO_3)_2](NO_3)_2$ (**1**), and one dimer, $[Np^{V}O_2(TEDGA)_2][Np^{VI}O_2(NO_3)_3].CH_3CN$ (**2**) using SC-XRD, Raman spectroscopy and DFT calculations. These compounds were prepared rationalizing the synthesis and mixing the monomers that form the complexes: $Np^{V}O_2(TEDGA)_2^+$ and $Np^{VI}O_2(NO_3)_2(H_2O)_2$ for the trimer and $Np^{VI}O_2(TEDGA)_2^+$ and $Np^{VI}O_2(NO_3)_3$ for the dimer. As these syntheses can be easily adapted to a wide range of systems, they open the way to the study of numerous CCI systems and the possibility of capitalizing on more and more data on these CCI compounds, which remain difficult to identify today. The comparison with the corresponding Np(V)-TEDGA monomer (**3**) $[NpO_2{}^{V}(TEDGA)_2].NO_3$ and Np(VI) di-nitrate structures, as well as the DFT calculations show that weak interactions within the CCI species have a strong influence on the shape of the CCI interaction and on the strength of the bond. Changing the length of the alkyl chains increases the cation-cation binding strength but this is not associated to an electronic donor effect from ethyl groups, but to weak interactions involving the DGA alkyl groups and oxygen or chloride atoms from $Np^{VI}O_2(A)_2$. Replacing nitrate by chloride anions increases the binding strength in association with a diminution of the cation-cation distance (Np^{VI}-O_{Np}) between neptunyl oxygen atoms. This is expected due the higher electronic charge on Np(VI) atom with chloride ions inducing stronger cation-cation interactions, as well as the reduced steric hindrance effects in the Np(VI) coordination sphere. The bond energy between the two actinides is thus correlated to the basicity of the donor yl group influenced as well by the counter ion and by the steric hindrance in the coordination sphere of the receptor.

---

[1] C. Walther, M.A. Denecke, "Actinide Colloids and Particles of Environmental Concern", *Chem. Rev.,* 2013, 113, 995-1015.

[2] K.E. Knope, L. Soderholm, "Solution and Solid-State Structural Chemistry of Actinide Hydrates and Their Hydrolysis and Condensation Products", *Chem. Rev.,* 2013, 113, 944-994.

[3] M. Altmaier, X. Gaono, T. Fanghanel, "Recent Advances in Aqueous Actinide Chemistry and Thermodynamics", *Chem. Rev.,* 2013, 113, 901-943

[4] L. Daronnat, V. Holfeltz, N. Boubals, T. Dumas, P. Guilbaud, D. Moreno Martinez, P. Moisy, S. Sauge-Merle, D. Lemaire, P. L. Solari, L. Berthon, C. Berthomieu, "Investigation of the Plutonium(IV) Interactions with Two Variants of the EF-Hand Ca-Binding Site I of Calmodulin", *Inorg. Chem.* 2023, 62, 21, 8334–8346.

[5] G. Chupin, C. Tamain, T. Dumas,P.L. Solari, P. Moisy, D. Guillaumont, "Characterization of a Hexanuclear Plutonium(IV) Nanostructure in an Acetate Solution via Visible-Near Infrared Absorption Spectroscopy, Extended X-ray Absorption Fine Structure Spectroscopy, and Density Functional Theory", *Inorg. Chem.* 2022 61(12), 4806-4817.

[6] P. Moeyaert, T. Dumas, D. Guillaumont, K.Kvashnina, C. Sorel, M. Miguirditchian, P. Moisy, J-F. Dufrêche, "Modeling and Speciation Study of Uranium(VI) and Technetium(VII) Coextraction with DEHiBA", I*norg. Chem.* 2016, 55, 13, 6511–6519

[7] M.J. Sarsfield , R.J. Taylor, C.J. Maher, "Neptunium(V) disproportionation and cation–cation interactions in TBP/kerosene solvent", Radiochim. Acta, 2007, 95, 677–682.

[8] R.G. Denning, "Electronic Structure and Bonding in Actinyl Ions and their Analogs", *J. Phys. Chem.* 2007, 111, 4125-4143.

[9] M. Basile, E. Cole, T.Z. Forbes, « Impacts of Oxo Interactions on Np(V) Crown Ether Complexes », *Inorg. Chem.,* 2018, 57, 6016-6028.
[10] C.R. Graves, J.L. Kiplinger, "Pentavalent uranium chemistry—synthetic pursuit of a rare oxidation state", *Chem. Comm.* 2009, 26, 3831-3953.
[11] D. L. Clark, S. D. Conradson, R. J. Donohoe, D. Webster Keogh, D. E. Morris, P. D. Palmer, R. D. Rogers, and C. Drew Tait, "Chemical speciation of the uranyl ion under highly alkaline conditions. Synthesis, structures, and oxo ligand exchange dynamics", *Inorg. Chem.* 1999, 38, 7, 1456–1466
[12] P. L. Arnold, "Single-Molecule Magnets: Uranyl steps in the ring", *Nat. Chem.,* 2012, 4, 967-969.
[13] V. Mougel, J. Pécaut, M. Mazzanti, "New polynuclear U(IV)–U(V) complexes from U(IV) mediated uranyl(V) Disproportionation", Chem Commun., 2012, 48, 868-870.
[14] T. W. Newton, F. B. Baker, "A Uranium(V)-Uranium(VI) Complex and Its Effect on the Uranium(V) Disproportionation Rate", *Inorg. Chem.*, 1965, 4, 1166-1170.
[15] T. Z. Forbes, C. Wallace, P. C. Burns, "Neptunyl compounds: Polyhedron geometries, bond-valence parameters, and structural hierarchy ", *Can. Mineral.,* 2008, 46, 1623–1645.
[16] S. Fortier, T.W. Hayton, "Oxo ligand functionalization in the uranyl ion (UO22+)", *Coord. Chem. Rev.* 2010, 254, 197-214.
[17] G. Nocton, P. Horeglad, J. Pecaut, M. Mazzanti, "Polynuclear Cation−Cation Complexes of Pentavalent Uranyl: Relating Stability and Magnetic Properties to Structure", *J. Am. Chem. Soc.* 2008, 130, 49, 16633–16645.
[18] V.N. Serezhkin, G.V. Sidorenko, D.V. Pushkin, L.B. Serezhkina, "Cation-cation interactions between uranyl(VI) ions", *Radiochemistry* 2014, 56(2), 115-133
[19] N.N. Krot, M.S. Grigoriev, "Cation–cation interaction in crystalline actinide Compounds", *Russ. Chem. Rev.*, 2004, 73, 89-99.
[20] M. S. Grigoriev, N.N. Krot, A.A. BEssonov, K.Y. Suponitsky, "Dimeric dioxocations, $(NpO_2^+)_2$, in the structure of bis(μ-2-fluorobenzoato)di-μ-oxo-bis[(2,2-bipyridine-N,N')oxoneptunium(V)]", *Acta Cryst Sect E*, 2007, E63, m561-562.
[21] A. Cousson, S. Dabos, H. Abazli, F. Nectoux, M. Pagès, « Crystal structure of neptunyl cation-cation complex (NpO2+) with mellitic acid : Na4(NpO2)2C12O12.8H2O », *J. Less Com Met,* 1984, 99, 233-240.
[22] M. S. Grigor'ev, I. A. Charushnikova, A. M. Fedoseev, "Molybdate Complexes of Np(V) with Outer-Sphere Cs+ Cations", *Radiochemistry,* 2021, 63, 133–140.
[23] M. S. Grigor'ev, I. A. Charushnikova, A. M. Fedoseev, "Molybdate Complexes of Np(V) with Li+ and Na+ Cations in the Outer Sphere", *Radiochemistry*, 2020, 62, 465–473.
[24] M. S. Grigor'ev, I. A. Charushnikova, A. M. Fedoseev, "Cation–Cation Interaction in the Np(V) Complex with Cyclobutanecarboxylic Acid Anions, Na[NpO2(cbc)2]", *Radiochemistry*, 2019, 61(4), 427–433.
[25] Zegke, G.S. Nichol, P.L. Arnold, J.B. Love, "Catalytic one-electron reduction of uranyl(VI) to Group 1 uranyl(V) complexes via Al(III) coordination", *Chem Comm*, 2015, 51, 5876-5879.
[26] J. Lhoste, N. Henry, P. Roussel, T. Loiseau, F. Abraham, « An uranyl citrate coordination polymer with a 3D open-framework involving uranyl cation-cation interactions", *Dalton Trans* 2011, 40, 2422-2424.
[27] D. Rose,Y-D. Chang, Q. Chen, J.Zubieta, "Reactions of Uranyl Thiolate Complexes with Molecular Oxygen: Syntheses and Crystal and Molecular Structures of the Uranyl Thiolate Peroxo Species (HNEt3)2[(UO2)2(O2)(SC4N2H3)4] and (HNEt3)[H(UO2)2(O2)(SC4N2H2Me)4].cntdot.Me2CO.cntdot.0.5Et3N and of the Uranyl Thiolate Oxo Cluster (HNEt3)2[(UO2)4(O)2(SC5NH4)6].cntdot.Me2CO*", Inorg. Chem*. 1994, 33, 23, 5167–5168
[28] D.P. Mills, O.J. Cooper, F.Tuna, E.J.L. McInnes, E.S. Davies, J.MacMaster, F. Moro, W. Lewis, A.J. Blake, S.T. Liddle, "Synthesis of a Uranium(VI)-Carbene: Reductive Formation of Uranyl(V)-Methanides, Oxidative Preparation of a $[R_2C{=}U{=}O]2+$ Analogue of the $[O{=}U{=}O]^{2+}$ Uranyl Ion (R = $Ph_2PNSiMe_3$), and Comparison of the Nature of U^{IV}=C, U^{V}=C, and U^{VI}=C Double Bonds", *J. Am. Chem. Soc*. 2012, 134, 10047−10054.
[29] R. Cea-Olivares, G. Canseco-Melchor, M.M. Moya-Cabrera, V. Garcia-Montalvo, J.G. Alvarado-Rodriguez, R.A. Toscano, "Complexation of the uranyl ion (UO2) 2+ with a tetraphenylimidodiphosphinate ligand: the first trinuclear uranyl complex comprising a double l2-oxo (UO2) bridge", *Inorg. Chem. Comm.*, 2005, 8, 205–207.
[30] J. C. Taylor, A. Ekstrom, and C. H. Randall, " Crystal and molecular structure of trimeric bis(1,1,1,5,5,5-hexafluoropentane-2,4-dionato)dioxouranium(VI)", *Inorg. Chem.* 1978, 17, 3285-3289;
[31] A.Ekstrom, H.Loeh, C.H.Randall, L.Szego, J.C.Taylor, "The preparation and properties of bis(1,1,1,5,5,5,-hexafluoro-2,4-pentanedionato) dioxo uranium(VI*)", Inorg. Nucl. Chem. Letter*, 1978, 14, 301-304
[32] L. Chatelain, V. Mougel, J. Pecaut, M. Mazzanti, «Magnetic communication and reactivity of a stable homometallic cation–cation trimer of pentavalent uranyl", *Chem Sci.,* 2012, 3, 1075-1079
[33] M.S. Grigor'ev, M.Y. Antipin, N.N. Krot, "Crystal Structure of a Double Np(V) Ammonium Propionate, $NH_4[(NpO_2)_3(C_2H_5COO)_4(H_2O)].3H_2O$", *Radiochemistry* 2006, 48(1), 6-10

[34] A.A. Bessonov, N.N. Krot, M.S. Grigoriev, V.I. Makarenkov, "Synthesis of New Crystalline Pu(V) Compounds from Solutions: VII. Synthesis and Study of MPuO2C2O4.nH2O with M = NH4 and Cs", *Radiochemistry*, 2005, 47(5), 468-471.

[35] S. Schöne, J. März, T. Stumpf, A. Ikeda-Ohno, "Mixed-valent neptunium oligomer complexes based on cation–cation interactions", *Dalton Trans.,* 2019, 48, 6700-6703.

[36] S. Nuzzo, J.Van Leusen, B. Twamley, J.A. Platts, P.Kogerler, R. Baker," Oxidation of uranium(IV) thiocyanate complexes: cation-cation interactions in mixed-valent uranium coordination chains", *Dalton Trans.,* 2019, 48, 6704-6708.

[37] S. M. Cornet, L. J. L. Haller, M. J. Sarsfield, D. Collison, M. Helliwell, I. May, N. Kaltsoyannis, "Neptunium(VI) chain and neptunium(VI/V) mixed valence cluster complexes", *Chem. Commun*. 2009, 917-919.

[38] I. Charushnikova, E. Bossé, D. Guillaumont, P. Moisy, "Crystal and Electronic Structure of a Mixed-Valent Np(IV)-Np(V) Compound: $[BuMeIm]_5[Np(NpO_2)_3(H_2O)_6Cl_{12}]$ », *Inorg. Chem.* 2010, 49, 2077-2082.

[39] V. Mougel, J. Pécaut, M. Mazzanti, "New polynuclear U(IV)–U(V) complexes from U(IV) mediated uranyl(V) Disproportionation", Chem Commun., 2012, 48, 868-870.

[40] V. Mougel, P. Horeglad, G. Nocton, J. Pécaut, M. Mazzanti, "Stable Pentavalent Uranyl Species and Selective Assembly of a Polymetallic Mixed-Valent Uranyl Complex by Cation–Cation Interactions", *Angew. Chem.* 2009, 48, 8477 –8480.

[41] V. Mougel, P. Horeglad, G. Nocton, J. Pécaut, M. Mazzanti, "Cation–Cation Complexes of Pentavalent Uranyl: From Disproportionation Intermediates to Stable Clusters", *Chem. Eur. J.* 2010, 16, 14365 – 14377.

[42] R. Copping, V. Mougel, C. Den Auwer, C. Berthon, P. Moisy, M. Mazzanti, "A tetrameric neptunyl(v) cluster supported by a Schiff base ligand", *Dalton Trans.*, 2012, 41, 10900-10902

[43] A. B. Yusov, I. A. Charushnikova, A. M. Fedoseev, A. A. Bessonov, "Synthesis and Structure of Crystalline Complexes of Np(V) with 1,10-Phenanthroline-2,9-dicarboxylic Acid. Complexation in Solution and Spectral Studies », *Radiochemistry*, 2014, Vol. 56, No. 2, pp. 134–144.

[44] M.P. Wilkerson, C.J. Burns, H.J. Dewey, J.M. Martin, D.E. Morris, R.T. Paine, B.L. Scott, "Basicity of Uranyl Oxo Ligands upon Coordination of Alkoxides", *Inorg. Chem.* 2000, 39 (23), 5277−5285.

[45] S.E. Gilson, P.C. Burns, "The crystal and coordination chemistry of neptunium in all its oxidation states: An expanded structural hierarchy of neptunium compounds", *Coordination Chemistry Reviews*, 2021, 445, 15, 213994-

[46] Y. Sasaki, G.R. Choppin, "Solvent extraction of Eu, Th, U, Np and Am with N, N'-dimethyl-N,N'-dihexyl-3-oxapentanediamide and it analogous compounds", *Anal. Sci.*, 1996, 12, 225-30.

[47] Y. Sasaki, Y. Sugo, S. Suzuki, S. Tachimori, "The novel extractant, diglycolamides, for the extraction of lanthanides and actinides in HNO_3-n dodecane system", *Solv. Extr. Ion Exch*.,2001, 19, 91-103

[48] Y. Morita, Y. Sasaki, T. Asakura, Y. Kitatsuji, Y. Sugo, T. Kimura, "Development of a new extractant and a new extraction process for minor actinide separation", *IOP Conf. Series: Mater. Sci. Eng*., 2010, 9, 012057

[49] R.B. Gujar, S.A. Ansari, P.K. Mohapatra, V.K. Manchanda, "Development of T2EHDGA based process for actinide partitioning. Part I: Batch studies for process optimization", *Solv. Extr. Ion Exch.*, 2010, 28, 350-66.

[50] D. Whittaker, A. Geist, G. Modolo, R. Taylor, M. Sarsfield, A. Wilden, "Applications of Diglycolamide Based Solvent Extraction Processes in Spent Nuclear Fuel Reprocessing, Part 1: TODGA*", Solvent Extr. Ion Exch*. 2018, 36, 223–256.

[51] S.A. Ansari, P. Pathak, P.K. Mohapatra, V.K. Manchanda, "Chemistry of Diglycolamides: Promising Extractants for Actinide Partitioning*", Chem. Rev.* 2012, 112, 1751–1772.

[52] S. Chapron, C. Marie, G. Arrachart, M. Miguirditchian, S. Pellet-Rostaing, "New Insight into the Americium/Curium Separation by Solvent Extraction Using Diglycolamides", *Solvent Extr. Ion Exch.* 2015, 33, 236–248

[53] Y. Sasaki, H. Suzuki, Y. Sugo, T. Kimura, G.R. Choppin, "New water-soluble organic ligands for actinide cations complexation", *Chem. Letters*, 2006, 35, pp.256-57

[54] X. Heres, P. Baron, Increase in the separation factor between americium and curium and/or between lanthanides in a liquid-liquid extraction process, 2011, Patent WO/2011/012579

[55] L. Klass, A. Wilden, F. Kreft, C. Wagner, A. Geist, P.J. Panak, I. Herdzik, J. Narbutt, G. Modolo, "Evaluation of the Hydrophilic Complexant N,N,N',N' -tetraethyldiglycolamide (TEDGA) and its Methyl-substituted Analogues in the Selective Am(III) Separation", *Solvent Extraction and Ion Exchange*, 2019, 37(5), 1-16

[56] M. Autillo, R.E. Wilson, M. Vasiliu, G. F. de Melo, D. A Dixon, « Periodic Trends within Actinyl(VI) Nitrates and Their Structures, Vibrational Spectra, and Electronic Properties », *Inorg Chem.*, 2022, 61(39), 15607-15618

[57] SAINTPlus; version 6.22; Bruker Analytical X-ray Systems: Madison, WI, 2001.

[58] SADABS, version 2.03; Bruker Analytical X-ray Systems: Madison, WI, 2001.

[59] Sheldrick, G. M. *Acta Crystallogr., Sect. A: Found. Crystallogr.* 2008, 64, 112−122.

[60] *Gaussian 16, Revision C.01*, 09, M. J. Frisch, G. W. Trucks, H. B. Schlegel, G. E. Scuseria, M. A. Robb, J. R. Cheeseman, G. Scalmani, V. Barone, G. A. Petersson, H. Nakatsuji, X. Li, M. Caricato, A. V. Marenich, J. Bloino, B. G. Janesko, R. Gomperts, B. Mennucci, H. P. Hratchian, J. V. Ortiz, A. F. Izmaylov, J. L. Sonnenberg, D. Williams-Young, F. Ding, F. Lipparini, F. Egidi, J. Goings, B. Peng, A. Petrone, T. Henderson, D. Ranasinghe, V. G. Zakrzewski, J. Gao, N. Rega, G. Zheng, W. Liang, M. Hada, M. Ehara, K. Toyota, R. Fukuda, J. Hasegawa, M. Ishida, T. Nakajima, Y. Honda, O. Kitao, H. Nakai, T. Vreven, K. Throssell, J. A. Montgomery, Jr., J. E. Peralta, F. Ogliaro, M. J. Bearpark, J. J. Heyd, E. N. Brothers, K. N. Kudin, V. N. Staroverov, T. A. Keith, R. Kobayashi, J. Normand, K. Raghavachari, A. P. Rendell, J. C. Burant, S. S. Iyengar, J. Tomasi, M. Cossi, J. M. Millam, M. Klene, C. Adamo, R. Cammi, J. W. Ochterski, R. L. Martin, K. Morokuma, O. Farkas, J. B. Foresman, D. Fox, 2016.

[61] S. Grimme, J. Antony, S. Ehrlich, and S. Krieg, "A consistent and accurate ab initio parametrization of density functional dispersion correction (DFT-D) for the 94 elements H-Pu" *J. Chem. Phys*., 2010, 132, 154104.

[62] L. Wittmann, I. Gordiy, M. Friede, B. Helmich-Paris, S. Grimme, A. Hansen,M. Bursch, "Extension of the D3 and D4 London dispersion corrections to the full actinides series", *Phys. Chem. Chem. Phys.,* 2024, 26, 21379-21394.

[63] X. Y. Cao, M. Dolg, H. Stoll, "Valence basis sets for relativistic energy-consistent small-core actinide pseudopotentials", *J. Chem. Phys.*, 2003, 118, 487-496.

[64] X. Y. Cao, M. Dolg, "Segmented contraction scheme for small-core actinide pseudopotential basis sets", *J. Mol. Struct.: THEOCHEM*, 2004, 673, 203-209.

[65] I. D. Brown, "Bond valences—a simple structural model for inorganic chemistry", *Chem. Soc. Rev.,* 1978, 7, 359–376.

[66] I. D. Brown, "Chemical and Steric Constraints in Inorganic Solids", *Acta Crystallogr.,* 1992, B48, 553-572.

[67] I. D. Brown, *The chemical Bond in Inorganic Chemistry. The Bond Valence Model;* Oxford University Press: New York, 2002.

[68] O. C. Gagne, F. C. Hawthorne, « Comprehensive derivation of bond-valence parameters for ion pairs involving oxygen », *Acta Crystallogr., Sect. B: Struct. Sci., Cryst. Eng. Mater.,* 2015, 71, 562–578.

[69] T. E. Albrecht-Schmitt, P. M. Almond, R. E. Sykora*,* "Cation−Cation Interactions in Neptunyl(V) Compounds: Hydrothermal Preparation and Structural Characterization of NpO2(IO3) and α- and β-AgNpO2(SeO3)", *Inorg. Chem*., 2003, 42, 3788–3795.

[70] Cambridge Data Base (version 2020)

[71] G. Tian, L. Rao, S. Teat, G. Liu, "Quest for Environmentally Benign Ligands for Actinide Separations: Thermodynamic, Spectroscopic, and Structural Characterization of UVI Complexes with Oxa-Diamide and Related Ligands", *Chem.-Eur. J.,* 2009, 15, 4172-4181.

[72] S. Kannan, M.A. Moody, C.L. Barnes, P.B. Duval, "Lanthanum(III) and Uranyl(VI) Diglycolamide Complexes: Synthetic Precursors and Structural Studies Involving Nitrate Complexation", *Inorg. Chem.*, 2008, 47, 4691-4695.

[73] G. Tian, L. Rao, S. Teat, "Formation, structure, and optical properties of PuO22 + complexes with N,N,N′,N′-tetramethyl-3-oxa-glutaramide", *Inorg. Chem. Commun*., 2014, 44, 32-36

[74] G. Tian, J. Xu, L. Rao, "Optical Absorption and Structure of a Highly Symmetrical Neptunium(V) Diamide Complex", *Angew. Chem*., 2005, 44, 6200–6203.

[75] T. Kawasaki, S. Okumura, Y. Sasaki, Y. Ikeda, "Crystal Structures of Ln(III) (Ln = La, Pr, Nd, Sm, Eu, and Gd) Complexes with N,N,N′,N′-Tetraethyldiglycolamide Associated with Homoleptic $[Ln(NO_3)_6)]_3$", *Bull. Chem. Soc. Jpn*, 2014, 87, 294-300.

[76] S. Okumura, T. Kawasaki, Y. sasaki, Y. Ikeda, "Crystal Structures of Lanthanoid(III) (Ln(III), Ln = Tb, Dy, Ho, Er, Tm, Yb, and Lu) Nitrate Complexes with N,N,N′,N′-Tetraethyldiglycolamide", *Bull. Chem. Soc. Jpn*, 2014, 87, 1133-1139.

[77] Md. A. Islam, M. Autillo, C. Poulin-Ponnelle, C. Tamain, H. Bolvin, C. Berthon, " Are Actinyl Cations Good Probes for Structure Determination in Solution by NMR?", *Inorg. Chem.,* 2023, 62, 28, 10916–10927.

[78] G. B. Jin, "Mixed-Valent Neptunium(IV/V) Compound with Cation–Cation-Bound Six-Membered Neptunyl Rings", *Inorg. Chem.* 2013, 52, 21, 12317–12319.

[79] T.Z. Forbes, P.C. Burns, "The role of cation–cation interactions in a neptunyl chloride hydrate and topological aspects of neptunyl structural units*", J. Solid State Chem* 2007, 180, 106-112.

[80] A. Bondi*, "van der Waals Volumes and Radii", J. Phys. Chem.* 1964, 68, 441-451.

[81] M. Alyapyshev, V. Babain, L. Tkachenko, V. Gurzhiy, A. Zolotarev, Y. Ustynyuk, I. Gloriozov, A. Lumpov, D. Darin, A. Paulenova, "Complexes of Uranyl Nitrate with 2,6-Pyridinedicarboxamides: Synthesis, Crystal Structure, and DFT Study", *Zeitschrift fur Anorganische und Allgemeine Chemie*, 2017, 643(9); 585-592

[82] J-C. Berthet, P. Thuéry, J-P. Dognon, D. Guillaneux, and M. Ephritikhine "Sterically Congested Uranyl Complexes with Seven-Coordination of the UO_2 Unit: the Peculiar Ligation Mode of Nitrate in $[UO_2(NO_3)_2(Rbtp)]$ Complexes", *Inorg. Chem*. 2008, 47, 15, 6850–6862

[83] I. A. Charushnikova, C. Den Auwer, "Crystal Structure of Two New Molecular Adducts of Uranyl Nitrate with 2,2'-6,2''-Terpyridine" *Russian Journal of Coordination Chemistry*, 2007, 33(1), 53–60

[84] J. L. Lapka, A. Paulenova, L. N. Zakharov, M. Y. Alyapyshev, V.A. Babain, "Coordination of uranium(VI) with N,N'-diethyl-N,N'- ditolyldipicolinamide " IOP Conf. Series: Materials Science and Engineering 9 (2010) 012029

[85] M. M. Pyrch, L. J. Augustine, J. M. Williams, S. E. Mason, T. Z. Forbes, "Use of vibrational spectroscopy to identify the formation of neptunyl–neptunyl interactions: a paired density functional theory and Raman spectroscopy study", *Dalton Trans.*, 2022, 51, 4772-4785

[86] M. L. McKee, M. Swart, "Study of Hg_2^{2+} and Complexes of NpO_2^+ and UO_2^{2+} in Solution. Examples of Cation−Cation Interactions", *Inorg. Chem.* 2005, 44, 20, 6975–6982

[87] G. Socrates, *Infrared and Raman Characteristic groups frequencies: Tables and Charts*, 3rd edition, John Wiley and Sons, 2001, New York.

[88] D.V. Kravchuk, R.E. Wilson, "Stoichiometric Lanthanide Compounds with Diglycolamides: A Synthetic Approach toward Understanding Rare-Earth Speciation in Solution", *Inorg. Chem.*, 2024, 63, 22049−22060

[89] L.J. Bellamy, *The Infrared Spectra of Complex Molecules: Volume Two Advances in Infrared Group Frequencies*. Springer Netherlands, 1980.

[90] D.V. Kravchuk, X. Wang, M.J. Servis, R.E. Wilson, "Structural Trends and Vibrational Analysis of N,N,N',N'–Tetramethylmalonamide Complexes Across the Lanthanide Series", *Eur. J. Inorg. Chem.*, 2024, 27 (6), e202300632.

[91] S.H.J. De Beukeleer, H.O. Desseyn, "Vibrational analysis of some transition metal complexes with deprotonated and neutral malonamide", *Spectrochimica Acta Part A: Molecular Spectroscopy,* 1994, 50 (14), 2291-2309.

[92] L. V. Volod'ko, L.T. Huoah, " The vibrational spectra of aqueous nitrate solutions", *J. Appl. Spectrosc.,* 1968, 9, 1100–1104.

[93] B.M. Rapko, B.K. McNamara, R.D. Rogers, G.J. Lumetta, B.P. Hay, "Coordination of Lanthanide Nitrates with N,N,N',N'-Tetramethylsuccinamide", *Inorg. Chem.,* 1999, 38 (20), 4585-4592.

[94] J-C.G. Bünzli, E. Moret, J-R. Yersin, "Vibrational Spectra of Anhydrous Lanthanum, Europium, Gadolinium, and Dysprosium Nitrates and Oxinitrates", *Helv. Chim. Acta,* 1978, 61 (2), 762-771.

[95] C. Tamain, M. Autillo, D. Guillaumont, L. Guérin, R. Wilson, C. Berthon, « Structural and bonding analysis in monomeric actinides(IV) oxalate from ThIV to PuIV. Comparison with the AnIV nitrate series », *Inorg. Chem.*, 2022, 61, 31, 12337–12348

[96] R.P. Scholer, A.E. Merbach, "Raman and Infrared Study of Hexamethylphosphoramide Complexes of Lanthanide Perchlorates", *Inorganica Chimica Acta*, 1975, 15, 15-20.

[97] G. B. Jin, S. Skanthakumar, L. Soderholm, "Three New Sodium Neptunyl(V) Selenate Hydrates: Structures, Raman Spectroscopy, and Magnetism", *Inorg. Chem.* 2012, 51, 3220−3230.

[98] S. Wang, J. Diwu, E. V. Alekseev, L. J. Jouffret, W. Depmeier, T. E. Albrecht-Schmitt, "Cation–Cation Interactions between Neptunyl(VI) Units" *Inorg. Chem.* 2012, 51, 13, 7016–7018

[99] B. Guillaume, G. M. Begun, and R. L. Hahn, "Raman Spectrometric Studies of "Cation-Cation" Complexes of Pentavalent Actinides in Aqueous Perchlorate Solutions*", Inorg. Chem.,* 1982, 21, 1159-1166

[100] P. A. Smith, S. M. Hickam, J. E. S. Szymanowski, and P. C. Burns, "Mixed-Valent Cyanoplatinates Featuring Neptunyl–Neptunyl Cation–Cation Interactions", *Inorg. Chem*. 2018, 57, 15, 9504–9514.